**Ring Walking/Oxidative Addition Reactions for the Controlled Synthesis of Conjugated Polymers**
**DOE Grant Number: DE-FG02-98ER14910**
**PI: Dr. Guillermo Bazan**

**Final Technical Report**

Contact Information:
Center for Polymers & Organic Solids
2512 Physical Sciences Building-North
University of California
Santa Barbara, CA 93106-5090
(805) 893-5538
E-mail: bazan@chem.ucsb.edu

Project Personnel: Ronald Bakus, graduate student; Xiaofeng Liu, postdoctoral researcher; JungHwa Seo, postdoctoral researcher; Huaping Li, postdoctoral researcher; Jinnie Myung, laboratory assistant.

Period of Performance: 06/01/08-12/31/11
Total Amount: $450,000

*Abstract*

Power conversion efficiencies of plastic solar cells depend strongly on the molecular weight characteristics of the semiconducting polymers used for their fabrication. The synthesis of these materials typically relies on transition metal mediated catalytic reactions. In many instances, the ideal structures cannot be attained because of deficiencies in these reactions, particularly when it comes to being able to achieve high number average molecular weights and narrow molecular weight distributions. Another important conjugated polymer structure of interest is one in which a single functional group is attached at the end group of the chain. Such systems would be ideal for modifying surface properties at interfaces and for labeling biomolecular probes used in fluorescent biosensors. To respond to the challenges above, our efforts have centered on the design of homogenous transition metal complexes that are easy to prepare and effective in carrying out living, or quasi-living, condensative chain polymerization reactions. The key mechanistic challenge for the success of this reaction is to force the insertion of one monomer unit at a time via a process that involves migration of the transition metal-containing fragment to one terminus of the polymer chain. Chain growth characteristics are therefore favored when the metal does not dissociate from the newly formed reductive elimination product. We have proposed that dissociation is disfavored by the formation of a π-complex, in which the metal can sample various locations of the electronically delocalized framework, a process that we term "ring-walking", and find the functionality where oxidative addition takes place. Success has been achieved in the nickel-mediated cross coupling reaction of Grignard reagents with aromatic halides by using bromo[1,2-bis(diphenylphosphino)ethane]phenylnickel. This reagent can yield poly(thiophene)s (one of the most widely used type of polymer in plastic solar cells) with excellent stereoregularity and molecular weight distributions with polydispersities that are consistent with a living polymerization sequence. Another important objective of this program concerned the use of these new catalysts and improved mechanistic insight for the synthesis of specific polymeric materials with prespecified properties.

*Detailed Progress Report*

The original goals stated in the research proposal center on the development of controlled catalytic methods for the synthesis of conjugated polymers of interest for emerging technologies, such as optoelectronic devices and biosensory technologies. The demonstration of how know in catalytic methods toward the synthesis of materials heretofore not attained was also an important metric of success. We are pleased that these objectives were indeed attained, as described in more detail below.

Polymerizations based on homogeneous transition metal catalysts are anticipated to be a key ingredient in the synthesis of advanced organic semiconducting materials for emerging optoelectronic applications. These metal-mediated reactions provide greatest control over the structural composition and the molecular weight characteristics of conjugated polymers typically used in plastic solar cells. Recent work has demonstrated that high efficiency solar cells *require* high molecular weight products.[1-3] Traditionally, conjugated polymers have been synthesized via step-growth polymerizations using coupling reactions such as Suzuki,[4,5] Heck,[6-8] Stille,[9-11] and Sonogashira,[12-14] which lead to polydispersity indices (PDIs) approaching 2.0 and high molecular weight only at high conversion, as per the work by Flory.

Much of our efforts centered on studying the chemistry and applications of 'hot' metal catalysts for use in the synthesis of conjugated polymers with narrow molecular weight distributions and specific end groups (see **Figure 1**).

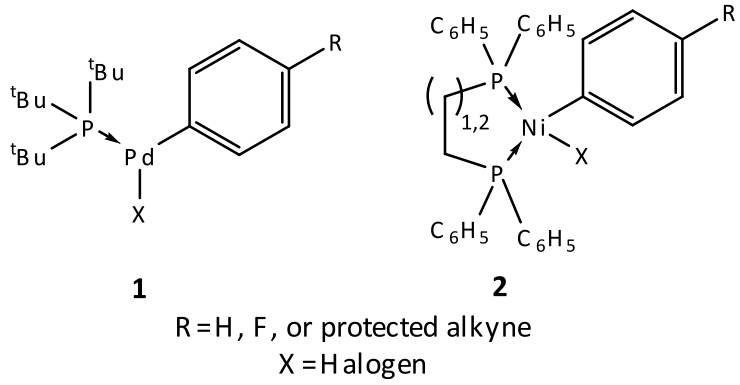


**Figure 1.** Representative catalysts studied, where **1** is a palladium catalyst for use in Suzuki polymerizations and **2** is a nickel catalyst for use in Grignard Metathesis (GRIM) polymerizations.

Molecules of the type in **Figure 1** are interesting because they can act as initiators for chain polycondensation polymerizations, where the aryl group bound to the metal center becomes attached to the end of growing polymer. The polymers generated typically have PDIs lower than that predicted by standard Flory statistics for condensation polymerizations. In addition, when R≠H, but is instead some masked functionality, it should become possible to selectively modify only one end of the polymer chain via post polymerization reactions, giving rise to novel materials that may have applications in DNA/protein biosensors, similar to previous work published by this group.[15]

*(a) The synthesis of* bromo[1,2-bis(diphenylphosphino)ethane]phenylnickel(II) *[4, (dppe)NiPhBr] (**4**),* bromo[1,2-bis(diphenylphosphino)ethane](4-fluorophenyl)nickel(II) *[4, (dppe)Ni(4-FPh)Br] (**5**), and the use of (dppe)NiPhBr and its fluorinated analogue in model polymerization studies of poly(3-alkylthiophene)s.*

Poly(3-alkylthiophene)s are an important synthetic target because their high charge carrier mobilities and absorption profiles make it a useful material for use in FETs and solar cells.[16,17] Until recently, the synthesis of regioregular, low polydispersity polythiophenes was challenging. McCullough demonstrated a simple system for generation of poly(3-alkylthiophene)s from readily available starting materials via nickel catalyzed cross-coupling procedure using [1,3-bis(diphenylphosphino)propane]nickel(II) dichloride [(dppp)$NiCl_2$], giving low polydispersity polymers (~1.2-1.6).[18] Unfortunately, the polymers generated are not mono-functional, leading to difficulties in selective post polymerization reactions.[19] Building on work by McCullough, we have obtained poly(3-dodecylthiophene) with PDIs as low as 1.07, and molecular weights ($M_n$) on the order of 74,000 g/mole using the initiator bromo[1,2-bis(diphenylphosphino)ethane]phenylnickel(II) (**4**, see **Scheme 1**). The initiator has the advantage of providing well-defined endgroups, with one active growing chain end, exceptionally low polydispersities, and excellent head to tail ratios for the resultant polymer (>98%).

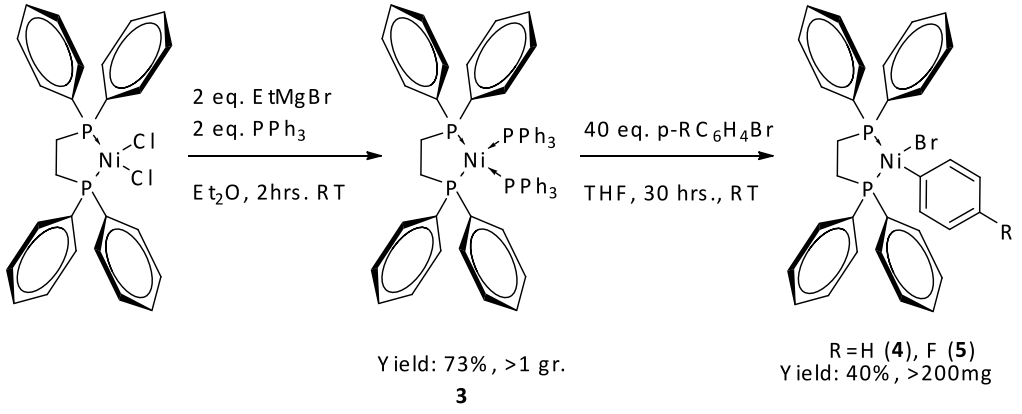


**Scheme 1**. Synthesis of initiators **4** and **5**.

Although compound **4** was reported once, it was not used for polymerization studies. When we attempted to reproduce the original synthetic method employed by Amatore and Jutand,[20] the yield was low, and purification proved to be difficult due to the impurities having very similar solubility's to that of the product. As such, a modified synthesis was used to allow for cheap, fast access to the target compound. Treatment of commercially available [1,2-bis(diphenylphosphino)ethane]nickel(II) dichloride [(dppe)$NiCl_2$] with ethylmagnesium bromide (EtMgBr) in the presence of two equivalents of triphenylphosphine gave [1,2-bis(diphenylphosphino)ethane]bis(triphenylphosphine)nickel(0) [**3**, (dppe)Ni$(PPh_3)_2$] in 73% yield. The crude powder obtained from this reaction was greater than 99% pure, as determined via $^1H$ and $^{31}P$ NMR spectroscopy, and used without further purification (trace bis[1,2-bis(diphenylphsophino)ethane]nickel(0) [$(dppe)_2Ni$] was detected, but proved inert in the next step, and was easily removed on workup of the target compound). The initiator species was then prepared by addition of a THF solution

containing (dppe)Ni($PPh_3$)$_2$ to 40 equivalents of either bromobenzene (to give **4**) or 1-bromo-4-fluorobenzene (to give **5**). The reaction was allowed to stir at ambient temperature for 24-30 hours, followed by removal of the THF under vacuum to give the initiators as a yellow-orange powder in suspension. The crude initaitors were collected by filtration, and after reprecipitation to remove trace starting aryl halide, were obtained in 40% yield as a fine yellow-orange powder. All structures were verified via $^{1}H$, $^{13}C$, $^{31}P$ NMR, elemental analysis, and X-ray diffraction (XRD) (**Figure 2**). Compounds **4** and **5** are soluble in THF, in contrast to the nearly insoluble (dppx)$NiCl_2$ catalysts (x=ethane or propane).

Crystallographic characterization of **4** and **5** (**Figure 2**) show that both possess square planar coordination geometries at the metal center, with P-Ni bond lengths that are distorted from the analogous (dppe)$NiBr_2$; the P-Ni bond trans to the Ni-Br bond is shortened (2.13Å compared to 2.16Å in (dppe)$NiBr_2$) and the Ni-P bond trans to the aryl ring is considerably longer (2.22Å), though the bite angle for all complexes are approximately 86°. The Ni-C bond for **4** is 1.99Å long, while **5** exhibits a 0.04Å shorter bond length as compared to **4**. The bulk of the phosphine ligand lies in the plane of the nickel center, forcing the plane of the aryl ring to lie perpendicular to the square plane of the nickel complex.

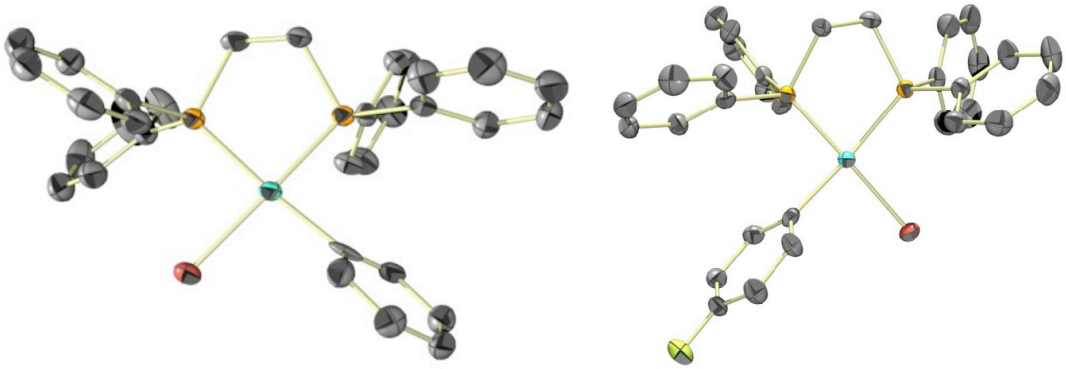

**Figure 2**. POV-Ray depiction of **4** and **5**, ellipsoids drawn at 50%, solvent and hydrogen atoms omitted for clarity.

Complexes **4** and **5** were screened as initiators for Grignard metathesis polymerization reactions. To a solution of either complex was added a solution containing a mixture of (5-bromo-4-dodecyl-2-thienyl)magnesium chloride·LiCl (**6**) and (5-bromo-3-dodecyl-2-thienyl)magnesium chloride·LiCl (**7**) monomers (prepared in situ by treatment of the 2,5-dibromo-3-dodecylthiophene premonomer with $^{i}$PrMgCl·LiCl), to give premonomer:catalyst ratio of 100:1. Upon addition of the monomer to the catalyst solution, an instant color change occurred from yellow to red for the solution. Formation of high molecular weight, low polydispersity poly(3-dodecylthiophene) was observed within 30 minutes. These results confirmed that complexes **4** and **5** were active for Grignard metathesis polymerization. The polymer's molecular weight could be tuned by simply changing the monomer loading, providing the ability to generate a series of conjugated polymers with varying molecular weight and a nearly monodisperse distribution for investigation of properties, see **Scheme 2**.

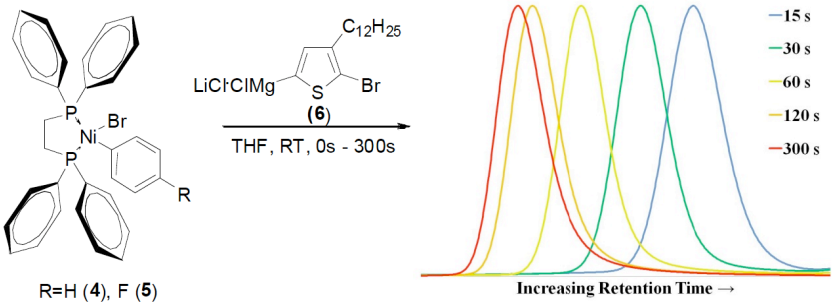


**Scheme 2.** Structure of **4** and **5** and GPC traces of poly(3-dodecylthiophene) initiated by **4**.

To investigate the kinetics of chain growth, the polymerization was carefully monitored over the course of 30 minutes using 1,4-dioctyloxybenzene as an internal standard. During polymerization, aliquots were removed at different time points and quenched using anhydrous p-toluenesulfonic acid. The resulting polymers were precipitated into ethanol and characterized by gel permeation chromatography (GPC) in THF. The supernatant was analyzed via GC-FID to determine the conversion. Analysis revealed that consumption of **6** (the 'active' isomer) is complete within 300 seconds (further discussion below), and a linear relationship between monomer conversion and polymer molecular weight was observed for the system (**Chart 1**). The polydispersity of each polymer remained low, with broadening only observed towards the end of reaction (**Table 1**). We observed that the slight molecular weight increase and broadening of the PDI after 300 seconds correlated with a small degree of consumption of (5-bromo-3-dodecyl-2-thienyl)magnesium chloride·LiCl (**7**, the 'less active' isomer). The combination of linear growth of molecular weight with monomer conversion and the extremely low polydispersity of the polymers support the assertion that the catalyst is operating in a quasi-living regime. When the ratio of premonomer:catalyst was increased to 400:1, a polymer of $M_n$ 74k with a PDI of 1.4 was obtained within 20 minutes. The unexpectedly low $M_n$ and broadened PDI are due to the presence of a low molecular weight tail, the origin of which remains unclear.

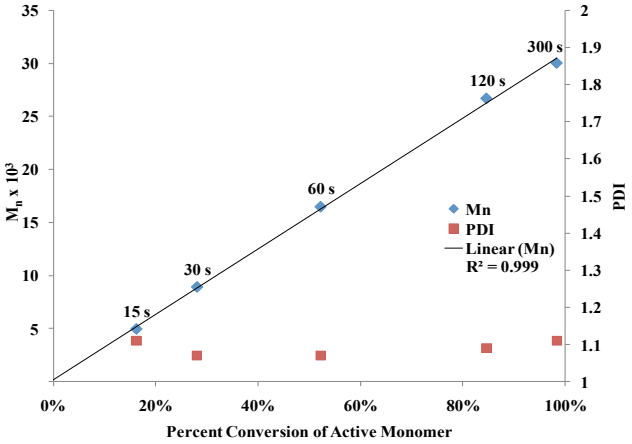


**Chart 1**. Plot of $M_n$ and PDI versus the conversion of active monomer.

| Entry/I[a]/T[b] | $M_n$[c] | PDI | Entry/I[a]/T[b] | $M_n$[c] | PDI |
|---|---|---|---|---|---|
| 1/**4**/15 s | 5.0 | 1.10 | 1a/**5**/15 s | 5.5 | 1.10 |
| 2/**4**/30 s | 8.9 | 1.07 | 2a/**5**/30 s | 10.2 | 1.08 |
| 3/**4**/60 s | 16.5 | 1.07 | 3a/**5**/60 s | 17.8 | 1.08 |
| 4/**4**/120 s | 26.7 | 1.09 | 4a/**5**/120 s | 26.3 | 1.10 |
| 5/**4**/300 s | 30.3 | 1.11 | 5a/**5**/300 s | 28.4 | 1.10 |
| 6/**4**/30 m | 33.0 | 1.20 | 6a/**5**/30 m | 30.1 | 1.17 |

**Table 1**. The development of polymer molecular weight versus time using initiators **4** and **5**. [a] Polymerizations carried out with 13.5 μmol of **4** (entries 1-6), 13.5μmol of **5** (entries 1a-6a); [b] Reaction time in seconds (approximate); [c] $M_n \times 10^3$ g·mol$^{-1}$ determined by GPC in THF at RT.

Analysis via matrix assisted laser desorption ionization-time of flight mass spectrometry (MALDI-TOF) of polymers generated with **4** do not display the required mass resolution to discriminate between Ph-/-H and Br-/-H terminated chains (**Figure 3**). However, polymers synthesized using initiator **5**, due to the increased mass of fluorine substitution, definitively show that the majority of polymers contain $FC_6H_4$-/-H termination (**Figure 3**). There is no evidence for Br or isopropyl groups being incorporated at the chain ends, indicating no premature chain termination of the catalyst during polymerization. $^1$H NMR spectroscopic analysis of the polymers confirm incorporation of the phenyl end group into the polymers, and show that the polymers are >98% head to tail regioregular.[21]

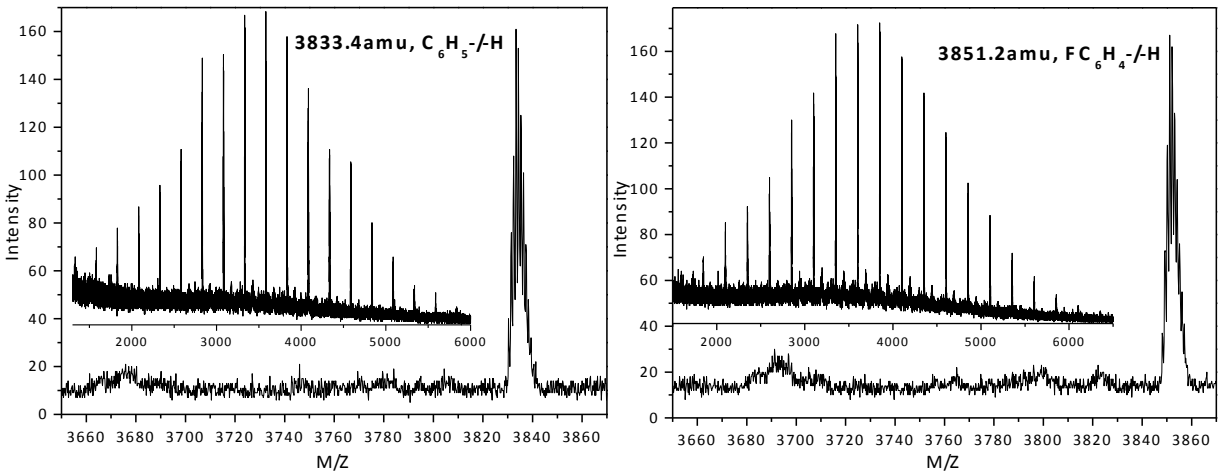


**Figure 3**. MALDI-TOF of poly(3-dodecylthiophene) initiated using **4** (left) and **5** (right).

Work by Achord and Rawlins[22] provides a useful point of reference to compare the rate of polymerization to our initiators. In their work, it is shown that for 1,3-bis(diphenylphosphino)propane nickel(II) chloride ((dppp)$NiCl_2$), at a similar concentration of 2,5-dibromo-3-hexylthiophene premonomer, near complete consumption of the monomer and maximum molecular weight is achieved in approximately 120 minutes. Although there is a difference in the length of the alkyl chains between their study and ours, this would not be expected to impact the rate of polymerization, and any difference in rate should be due to the catalyst. Their observation that monomer consumption is nearly complete after 120 minutes differs significantly from what was observed with our system. The approximately twenty fold rate increase over their reported data for (dppp)$NiCl_2$ (complete consumption of the monomer

and maximum molecular weight in 300 seconds), offers a clue as to previous reports that showed reactions using (dppe)$NiCl_2$ to result in broader PDI distributions with lower molecular weight than (dppp)$NiCl_2$.[23] We believe that this a consequence of the extremely rapid rates of the (dppe)$Ni^{(0)}$ propagating species compared to (dppp)$Ni^{(0)}$, and the initial heterogeneous nature of the (dppx)$NiCl_2$ systems in THF (x=e or p). The initiating step for the Grignard metathesis cycle is the reduction of the starting $Ni^{(II)}$ to $Ni^{(0)}$. Because of the relative insolubility of the starting (dppx)$NiCl_2$, the reduction proceeds via a solid-liquid phase reaction, which is inherently slower than the analogous homogeneous reaction.[24] Upon reduction, the soluble nickel species can participate in the catalytic cycle. This slow initiation step can lead to PDI broadening.[25]

Additionally, use of (dppp)$NiCl_2$ to generate poly(3-hexylthiophene) (P3HT) suffers from the tendency for P3HT to precipitate from the common solvents used in Grignard metathesis, once sufficiently high molecular weight is achieved, placing practical limits on the control of molecular weight. Our system shows a tendency to reach a molecular weight maximum more quickly than dppp based systems, and thus we were interested to determine if higher molecular weights could be achieved as compared to the dppp based systems by outpacing the process of precipitation. Under similar conditions to those previously mentioned, we obtained P3HT of $M_n$ 24k and 41k, with PDI 1.2 and 1.15 respectively, when using 100 and 200 eq. of the premonomer. Precipitation of the polymer did not become apparent until 10-15 minutes after initiation, whereas maximum molecular weight should have been achieved in 5-10 minutes, based on the results from the 3-dodecylthiophene polymerizations.

The low PDI and linear molecular weight increase versus monomer conversion closely resemble what one would expect from a traditional living polymerization, *i.e.* living anionic polymerizations. In living anionic polymerizations, the growth of the polymer occurs from only one end of the polymer (the active site), with all chain ends actively growing at the same time (no termination reactions). For GRIM systems to operate in this quasi-living regime, similar constraints also apply, *i.e.* all chains actively growing at the same time (no dissociation from the active growing chain end), and from only one chain end. One can rationalize this in light of the proposed mechanistic cycle below (**Figure 4**). Entry of **4** into the catalytic cycle occurs via transmetalation of nickel with the thiophene Grignard, which rapidly undergoes reductive elimination, giving a phenyl endcapped thiophene bromide species. The eliminated (dppe)nickel$^{(0)}$ species is coordinatively unsaturated and satisfies the coordinative unsaturation by remaining associated with the π-system of the polymer chain (probably via some $d \rightarrow \pi^*$ dative bonding mode). The catalyst then ring walks across the π-system, and rapidly undergoes oxidative addition to the thiophene-bromine bond, turning over the catalyst and allowing for addition of another monomer unit. Exit from the cycle could result from dissociation of the nickel species from the growing chain end, or via termination of the growing chain end via a proton source.

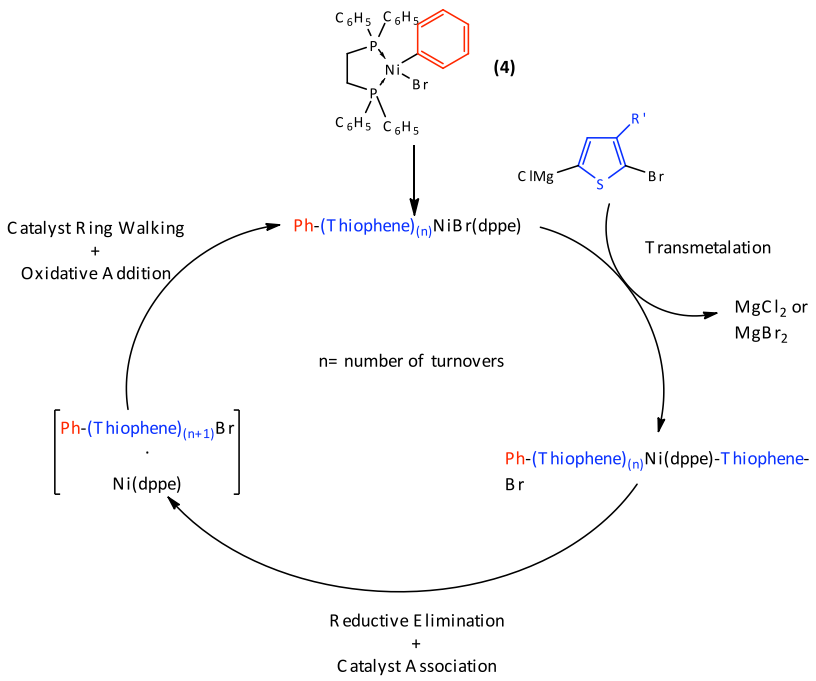


**Figure 4**. Proposed catalytic cycle for **4**.

Thus, compound **4** can be used as a catalyst for Grignard metathesis polymerization, which rapidly provides high molecular weight poly(thiophene)s, $M_n$=30k-74k, with polydispersity between 1.1-1.4, and through the inclusion of an initiating moiety, selectively functionalizes one end of the polymer. Since McCullough has demonstrated the possibility of end capping the polymer chain at the end of the polymerization,[26] it is likely that by using these initiating moieties and end capping at the end of the polymerization, it will be possible to generate bifunctional polymers.

*(b) Application of Compound **4** for the Synthesis of Selectively Functionalized Conjugated Polymers for Biosensory Applications.*

Based on the reactivity of compound **4**, it occurred to us that it would be possible to access conjugated polymer structures with up to now unattainable molecular structures and therefore unique physical properties. An ideal conjugated polymer for biosensor applications would have the following desirable attributes: high photoluminescence quantum yield, water-solubility, uniformity in chain length, resistance to non-specific interactions, and a single-site for bio-recognition. To the best of our knowledge such materials have not been reported and their preparation would require taking full advantage of modern polymer synthesis techniques.

Fluorene-based polymers usually provide superior emission characteristics over thiophene-based materials, especially in aqueous media, but metal-halogen exchange is slower for 2,7-dibromo-9,9-dialkylfluorene systems, often requiring more than 8 hours to form the active metalated species. Furthermore, this treatment can result in unreacted alkyl Grignard in solution or the generation of bis-metalated fluorene species, both of which hinder chain growth characteristics.[27] In contrast, it has been shown that 2-bromo-7-iodofluorene pre-monomers subjected to similar conditions undergo metal-halogen exchange exclusively with iodide,

generating the mono-metalated active species within one hour.[28] Therefore, a 2-bromo-7-iodofluorene core was selected for our study.

Fluorene repeat units with oligo(ethylene glycol) side chains were targeted to generate the requisite aqueous polymer solubility. The length of solubilizing oligo(ethylene glycol) group required some consideration: a chain which was too short would not provide the necessary solubility, whereas one that was too long would dilute the emissive component of the material and could potentially interfere with substrate binding. Fluorene-phenylene polymers containing alternating tri(ethylene glycol) monomethyl ether and tri(ethylene glycol) *tert*-butyl ester side chains show good organic solubility, but are not completely water soluble.[29] 2-Bromo-7-iodo-fluorene with octa(ethylene glycol) monomethyl ether chains at the 9,9'-positions was therefore selected. The octa(ethylene glycol) chain was synthesized from two tetra(ethylene glycol) subunits,[30] as illustrated in **Scheme 3**. First, tosyl groups were installed on both ends of tetra(ethylene glycol) by treatment with tosyl chloride to give the bis(tosylate) **8**.[31] Tetra(ethylene glycol) monomethyl ether was then deprotonated with sodium hydride and slowly added to a THF solution of **8** to yield octa(ethylene glycol) monomethyl ether tosylate, **9**.[32] Conversion of the terminal tosyl group to iodide gave **10**.[33] Treatment of 2-bromo-7-iodo-fluorene with potassium hydride in THF, followed by addition of **10** afforded the pre-monomer **11** in good yield.

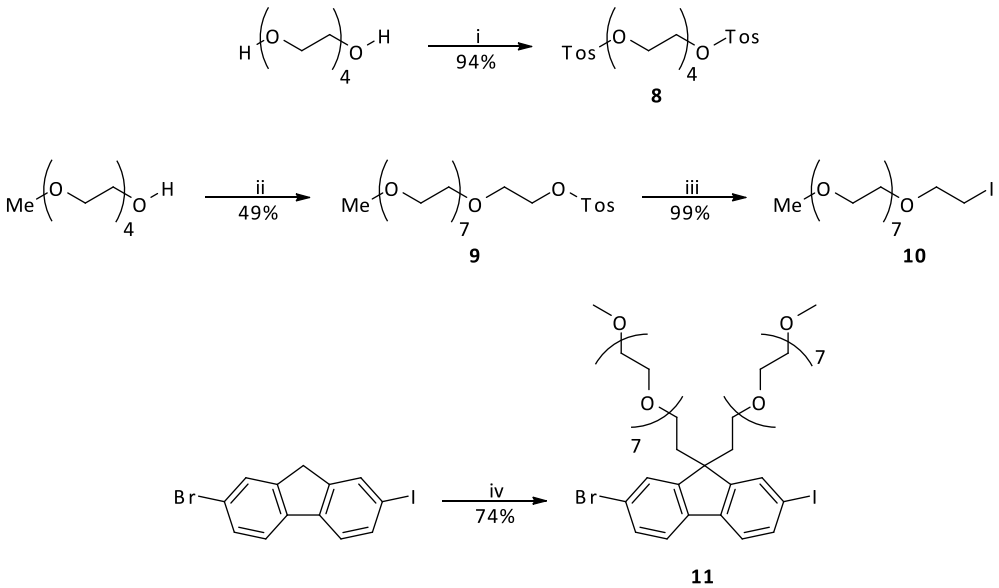


**Scheme 3.** Synthesis of pre-monomer **11**. Synthetic conditions: i) tosyl chloride, triethylamine, ether, 0ºC – RT, 18 hrs; ii) (a) NaH, THF, 2 hrs, (b) **8**, THF, 19 hrs; iii) NaI, acetone, reflux, 15 hrs; iv) (a) KH, THF, 1.5 hrs, (b) **10**, THF, 14 hrs.

The polymerization of fluorene-based monomers is more challenging than that of the thiophene counterparts. Thus, our subsequent studies focused on the polymerization of **11**, as shown in **Scheme 4**. Treatment of **11** with isopropylmagnesium chloride-lithium chloride complex at -35ºC for 40 minutes resulted in formation of the reactive species which, in the presence of (dppe)Ni(Ph)Br, quickly polymerized (< 30 sec) to give the product as a yellow-green, waxy solid. Purification was achieved through selective precipitation and extraction procedures that took advantage of the high solubility of the product in solvents such as $CH_2Cl_2$

and toluene, and its insolubility in hexane. With a monomer to catalyst ratio of 40:1, GPC analysis (DMF, 0.01% LiBr, calibrated against polystyrene standards) provided a number-average molecular weight ($M_n$) in the 26 and 30 kDa range with PDI values of 1.3 – 1.4. It is well known that discrepancies can exist between the true molecular weight and that as measured by GPC.[34] The polymer molecular weight was therefore measured by dynamic light scattering (DLS) techniques in DMF, to obtain a value of 32 kDa, which is similar to that obtained by GPC. The number of repeat units can therefore be estimated using $M_n$ and the mass of each repeat unit (897 g/mol) to give a DP of between 29 and 33. Extension of the polymerization time beyond 30 sec yielded only minimal gains in molecular weight at the expense of broader PDI values.

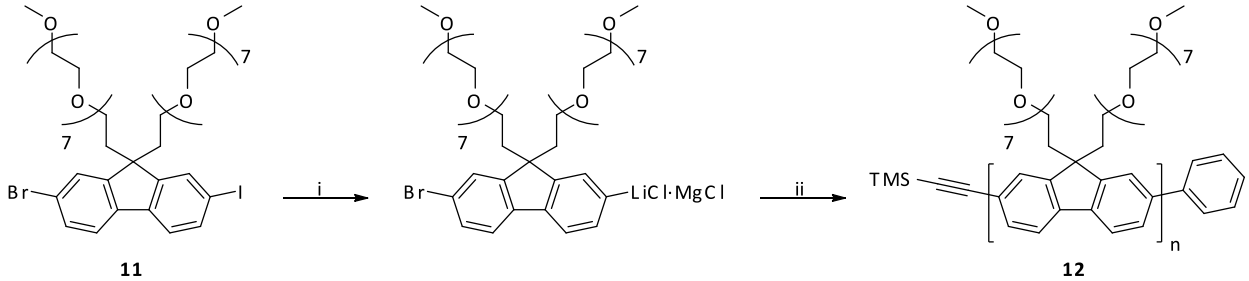


**Scheme 4.** Polymerization and end-functionalization of **11**. Synthetic conditions: i) *i*PrMgCl•LiCl, THF, -35ºC, 40 min; ii) (a) (dppe)Ni(Ph)Br (**4**), RT, 20 sec, (b) 2-trimethylsilylethynylmagnesium bromide, THF, 1.5 hrs.

Quenching of polymerizations of **11** with 2-trimethylsilylethynylmagnesium bromide was carried out to examine the efficiency of introducing a silylacetylene end group, as shown in Scheme 3. $^1$H NMR analysis of the purified product revealed three resonances between 8.0 and 7.8 ppm, which correspond to the three unique aromatic proton environments.[35] Signals due to the methylene protons from the pendant oligo(ethylene glycol) chains appear between 3.6 and 2.6 ppm[36] and the singlet attributed to the trimethylsilyl-protected ethynyl group appears at 0.28 ppm.[37] These data are consistent with the structure of the product **12** in **Scheme 4**. An estimate of end-group incorporation was calculated to gauge the efficiency of this procedure. A 29 kDa polymer (as measured by GPC) should contain approximately 32 units. Each aromatic $^1$H NMR resonance accounts for 2 protons on the repeat unit and therefore, a polymer with 32 repeat units should give rise to an integrated value of 64 protons for each aromatic resonance. For 100% end-group incorporation, the trimethylsilyl group should integrate for 9 H, and a ratio of TMS-ethynyl to each aromatic resonance of 9:64 or 0.14 should result. The $^1$H NMR spectrum of **12** gives an integral ratio of 8:64 or 0.125 from resonances at 0.28 ppm (trimethylsilylethynyl end group) and 8.0 ppm (one set of backbone aromatic protons), respectively. Division of this experimental value by the theoretical maximum, as calculated above, reproducibly demonstrated 80 – 90% acetylene end group incorporation into the polymer. End group incorporation was further confirmed using MALDI-TOF mass spectrometric analysis of a low molecular weight oligomer, prepared in a similar way to the polymer but with a higher initiator:monomer ratio. The resulting mass distribution exhibits peaks at 1968.0, 2864.4, and 3761.9 amu, corresponding to n = 2, 3, and 4 fluorene repeat units (MW = 896.51), respectively, with phenyl and TMS-ethynyl end groups. These data confirm the presence of the desired end groups on the majority of product. Optimization studies showed that success of end group incorporation depends on the polymerization time and decreases if the terminating Grignard reagent was added more than 30

seconds after initiation. Therefore, care was taken to determine the optimal polymerization time (20 sec) that achieved high molecular weight polymer, while still retaining satisfactory end-group incorporation.

Polymer **12** is soluble in polar organic solvents, including $CH_2Cl_2$, $CHCl_3$, methanol, ethanol, acetonitrile, and toluene. Furthermore, it can be dissolved in water and aqueous buffer solutions. **Figure 5** shows the UV-Vis absorption and emission properties in water, which are similar to those of other poly(fluorene)s.[38] Solutions of **12** display a broad absorption peak with a maximum ($\lambda_{max}$) at 387 nm in $CHCl_3$, while the $\lambda_{max}$ for aqueous solutions occurs at 405 nm, with a shoulder at 387 nm; the extinction coefficient is on the order of $4 \times 10^4$ $M^{-1}$ $cm^{-1}$, as calculated per repeat unit. Solution state photoluminescence measurements reveal a quantum yield of 0.8 in aqueous solution, which is comparable to other highly-efficient water-soluble fluorene-based polymers.[39,40] Emission maxima are located at 420 nm in $CHCl_3$ and 425 nm in water.

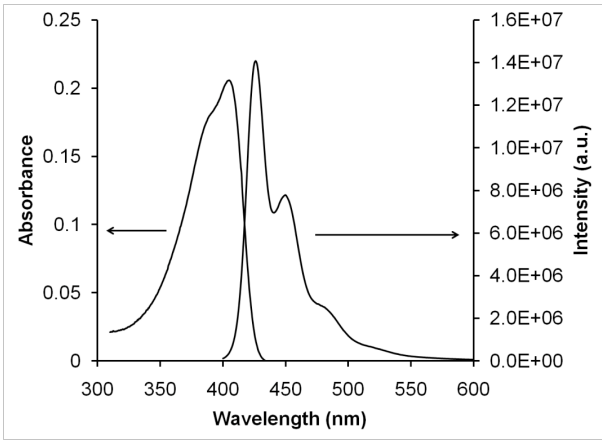


**Figure 5.** Absorption (left) and photoluminescence (right) spectra of polymer **12** in water.

The copper-catalyzed azide-alkyne cycloaddition reaction[41] is one type of Click chemistry[42] that is useful for installing a wide variety of functionalities to organic compounds bearing alkyne or azide moieties.[43] Several biologically-relevant organo-azides are commercially available, or can be readily synthesized, therefore this reaction was a logical choice for attaching relevant functional probes. Typical reactions involve a terminal alkyne[44] and thus, it was necessary to deprotect the terminal group of polymer **12**. De-silylation of this alkyne can be accomplished by treatment of **12** with potassium carbonate in methanol,[45] as illustrated in Scheme 4 to yield the deprotected alkyne-bearing polymer **13**. **Figure 6** depicts a comparison of the upfield region (0.5 – 0 ppm) for the $^1$H NMR spectra of **12** and **13**. It is evident that product **13** lacks the signal from the terminal trimethylsilyl protons, as was seen in that of **12**; no differences in polymer solubility before and after de-silylation were observed.

After deprotection, the terminal alkyne of **13** is active for Click chemistry. To determine an approximate yield of this final step, polymer **13** was treated with a test reagent, 3-azidopropyltrimethylsilane, in the presence of Cu(II)/sodium ascorbate in a THF/$H_2O$/*tert*-butanol solution[46] to give triazole-coupled product **14**, as shown in **Scheme 5**. This test reagent was selected to provide a unique signal in the $^1$H NMR spectrum that can be used to determine reaction efficiency. Furthermore, GPC measurements of **12**, **13**, and **14** showed no major differences in $M_n$ or PDI, indicating no change in the hydrodynamic volume of polymer due to potential undesirable side reactions. Therefore, a ratio was calculated between $^1$H NMR

integrated intensities from the appended TMS-containing test reagent and backbone aromatic proton resonances in **14**. Polymers **12** and **14** each contain a terminal trimethylsilyl moiety, the former from initial *in situ* end-functionalization and the latter from the final Click reaction. The ratio of integrated $^1$H NMR peak intensity between TMS-ethynyl and one set of backbone aromatic protons in **12** was compared to the ratio obtained for **14**, and the values were found to be virtually identical (0.125 vs. 0.120), indicating near quantitative conversion and successful post-polymerization incorporation of azide-containing organic reagents.

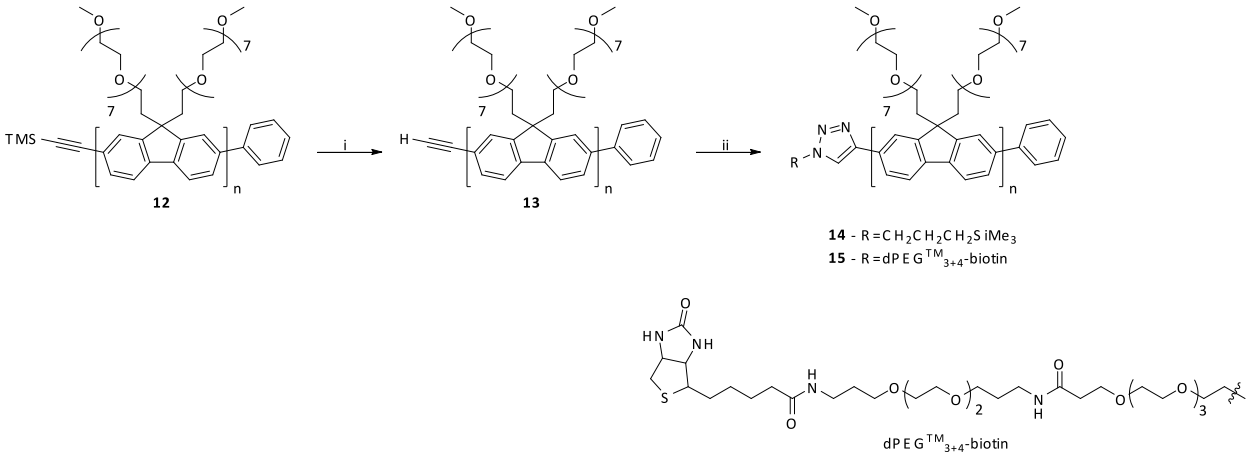


**Scheme 5**. Post-polymerization Click conjugation of **12**. Synthetic conditions: i) $K_2CO_3$, methanol, RT, 5 hrs; ii. R-$N_3$, $CuSO_4$•$5H_2O$/sodium ascorbate, THF/*tert*-butanol/$H_2O$, RT, 24 hrs..

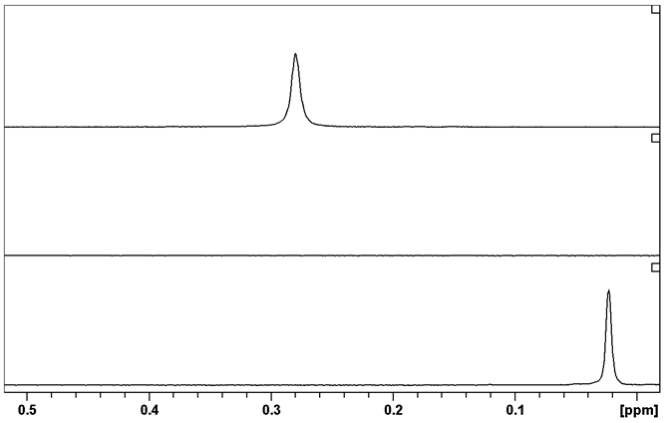


**Figure 6.** $^1$H NMR spectra (0.5 – 0 ppm) of **12** (top), **13** (middle), and **14** (bottom), highlighting deprotection of trimethylsilyl-ethynyl end-group of **12** (0.28 ppm) and subsequent Click reaction of **13** with 3-azidotrimethylsilane to generate **14** (0.02 ppm).

To demonstrate the applicability of this system to biosensing and imaging applications, it was necessary to attach an appropriate model reagent to the chain end, so as to provide a handle for studying probe-target specificity. For this purpose, we chose the biotin-streptavidin interaction, which is one of the strongest non-covalent interactions,[47] and is often utilized as a model for biosensor applications[48,49] and as an affinity pair in standard bio-assays.[50,51] Furthermore, derivatized streptavidin proteins and azide-containing biotin reagents are

commercially available. As shown in **Scheme 5**, using a procedure similar to that for the preparation of **14**, biotin-dPEG$^{TM}_{3+4}$-azide[52] (an azide-containing biotin with an oligo(ethylene glycol)) was reacted with polymer **13** and the product, **15**, was purified by dialysis against methanol. GPC analysis of **15** revealed no major differences in $M_n$ or PDI, relative to **12** or **13**. No resonances specific to the appended biotin moiety were observed in the $^1$H NMR spectrum of **15**, likely due to overlap with polymer resonances and therefore, NMR spectroscopy was unsuitable for determination of conjugation success. However, Fourier transform infrared spectroscopy (FT-IR) bands specific to the biotin fragment were useful in demonstrating attachment (**Figure 7**). The FT-IR spectrum of precursor polymer **13** contains bands near 1650 and 1600 cm$^{-1}$; after the Click reaction, new bands at 1710 and 1660 cm$^{-1}$ are observed which are assigned to carbonyl signals from biotin[53] and amide groups in the linker. Additionally, no azide stretch was evident at 2100 cm$^{-1}$, verifying removal of all unbound biotin reagent.

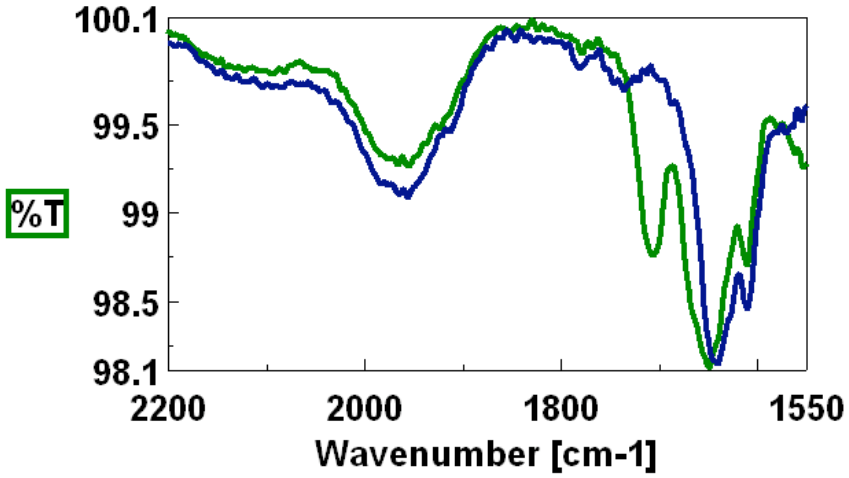


**Figure 7.** Comparison of FT-IR spectra of **13** (blue) and **15** (green), highlighting new carbonyl bands (1708, 1658 cm$^{-1}$) in **15** from successful attachment of biotin reagent. The absence of the azide stretch (2100 cm$^{-1}$) indicates efficient removal of starting material.

The ability of the biotin-functionalized polymer terminus of **15** to bind to a streptavidin receptor was used as a model assay to determine specific probe-analyte interactions. Streptavidin conjugates with appended chromophores are commercially available and were used to establish binding through fluorescence resonance energy transfer (FRET) experiments. FRET is a non-radiative transfer of energy from a donor absorbing moiety to an acceptor fluorophore.[54] A typical experiment involves excitation of a donor, followed by energy transfer to and emission by the acceptor, resulting in donor emission quenching and sensitization of acceptor luminescence. The efficiency of energy transfer is related to the spectral overlap between the donor and acceptor, but more importantly for the purpose of our experiments, is dependent on the spatial distance between the two and thus, is useful for verification of binding interactions.[55,56] Typical effective FRET distances range between 1 and 10 nm, as energy transfer efficiency decays as $1/r^6$, with r being the distance between donor and acceptor.[57] A streptavidin reagent with appended Alexa Fluor®-488 organic dye molecules (5 mol dye per mol Streptavidin) was selected as the binding partner due to suitable overlap between the emission of **15** and the absorption of the dye ($\lambda_{max,\ abs}$ = 495 nm, $\lambda_{max,\ em}$ = 520 nm). Binding between

streptavidin and the terminal biotin of **15** should bring the optical partners into close proximity, resulting in efficient FRET. The overall process is illustrated in **Scheme 6**. In contrast, no interaction should exist between a control polymer (**12** or **14**) and streptavidin.

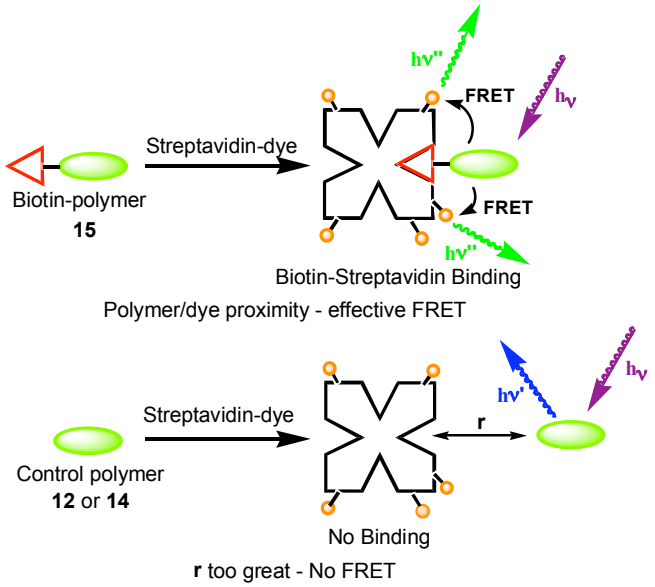


**Scheme 6.** Schematic for FRET detection of binding between **15** and Streptavidin-Alexa Fluor®-488 (5 mol dye/mol Streptavidin).

Thus, a solution of **15** (172 nM, calculated in terms of polymer chains, based on the $M_n$ from GPC) in Tris buffer was treated with aliquots of the streptavidin-Alexa Fluor®-488 dye conjugate (8.6 nM, calculated per protein molecule). As shown in **Figure 8**, before streptavidin-dye addition, excitation at 405 nm gave a typical polymer emission spectrum with a maximum near 425 nm. After introduction of one aliquot of streptavidin-dye, reduced polymer emission was observed with concomitant appearance of dye emission at 520 nm. The solution was treated with another aliquot of streptavidin-dye and further attenuated polymer emission and dye luminescence enhancement can be observed. This process, shown in **Figure 8**, was repeated until no further decrease in polymer luminescence or increase in dye emission was detected and the solution concentration of streptavidin-dye was noted (34.4 nM). It is known that streptavidin is a tetrameric protein capable of binding up to four biotin molecules[58] and thus, the concentration of biotin-binding sites should be equal to four times that of streptavidin protein molecules. The saturation concentration of streptavidin for this experiment, after which no further change in FRET was observed, therefore corresponds to an equivalent biotin-binding site concentration of 138 nM (i.e. 34.4 nM× 4).[59] A comparison of this biotin-binding site concentration relative to the concentration of polymer chains in solution (172 nM) gives a ratio of ~0.8. As noted earlier, GPC data and $^1$H NMR spectra of **12** are consistent with approximately 80 to 90% trimethylsilyl-ethynyl end-group incorporation. Comparison between the NMR spectra of **12** and **14** indicates nearly quantitative Click reactivity of this terminal alkyne, and therefore, approximately 80 – 90% of polymer chains of **15** should contain a biotin-termination. Thus, the ratio of streptavidin-bound polymer calculated from the FRET experiment (0.8) is approximately equal to the ratio of biotin-terminated polymer estimated from

$^{1}$H NMR spectroscopy and GPC data (0.8-0.9), indicating excellent end-group binding activity. An appropriate control experiment was performed using a polymer which contained no biotin-terminus, **12** or **14** (**Scheme 6**). As anticipated, addition of streptavidin-dye to a solution of **12** or **14** gave rise to no significant polymer emission quenching or dye luminescence upon excitation at 405 nm (Supporting Information). The absence of energy transfer between **12** or **14** and the streptavidin-dye conjugate highlights the resistance of these polymers to non-specific interactions.

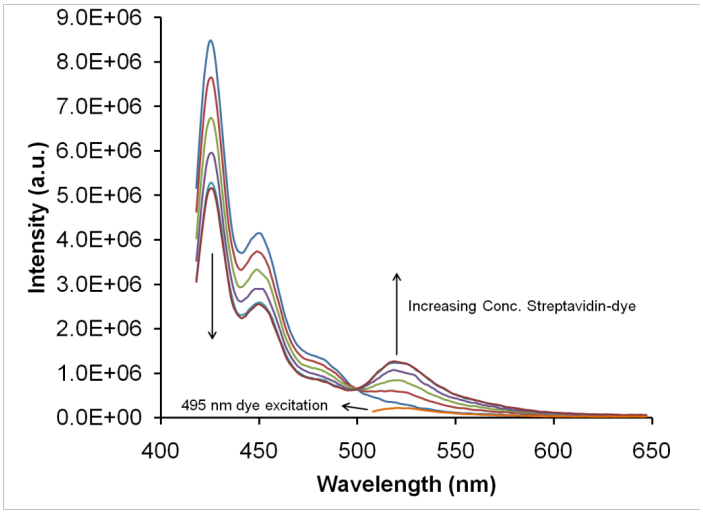


**Figure 8.** Fluorescence resonance energy transfer (FRET) from **15** (172 nM, excitation at 405 nm) to Streptavidin-Alexa Fluor®-488 (8.6 nM aliquots) showing decreased polymer emission (425 nm) and increased dye emission (520 nm) with increasing Streptavidin-dye concentration. Saturation of dye emission was observed after addition of four aliquots (34.4 nM Streptavidin-dye). The orange spectrum at bottom corresponds to emission from direct dye excitation (495 nm) for highest Streptavidin-Alexa Fluor®-488 concentration, highlighting signal enhancement due to FRET from **15**.

Another type of test was devised to examine the surface binding reactivity[60] of the biotin-terminus of polymer **15**. Streptavidin-functionalized cross-linked agarose beads were incubated with a solution of **15** (or **12**, as a control). Upon removal of non-bound polymer, beads treated with **15** were highly luminescent under UV excitation, whereas no luminescence was observed for samples treated with **12**. Confocal microscopy images of individual particles confirmed this observation. Beads treated with **15** or **12** were imaged under bright field illumination and in luminescence mode using 405 nm laser excitation. **Figure 9A** shows that beads treated with **15** exhibit blue emission. However, no luminescence was observed for those control particles treated with **12** (**Figure 9C**). **Figure 9B** displays the emission from a batch where emissive (treated with **15**) and non emissive (treated with **12**) beads were mixed together. Thus, polymers such as **15** provide well defined systems that are reactive for binding in solution and on surfaces and hold promise as luminescent reporters for a number of biological recognition applications.

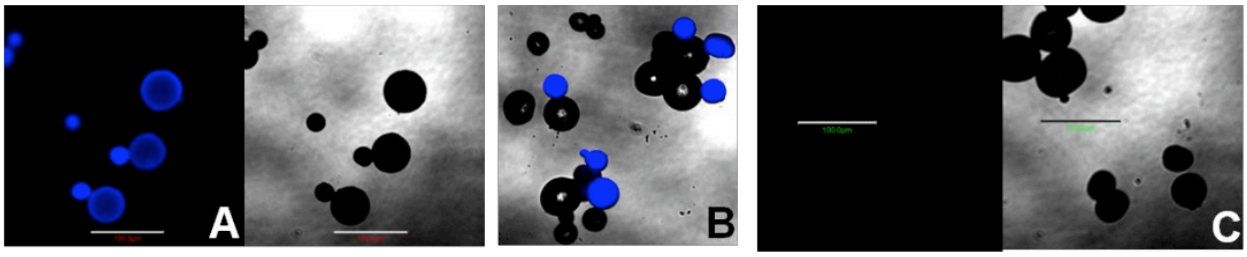


**Figure 9.** Confocal microscope images of streptavidin-coated beads treated with **15** (A) or **12** (C) captured in luminescence mode (left panel) or with bright field illumination (right panel). Middle image (B) is an overlay of luminescence and bright field images for a mixture of both sets of beads, showing emission from beads treated with **15** but no emission is visible from beads treated with **12**. Scale bar corresponds to 100 μm.

The work herein shows that it is possible to take advantage of monomer and catalyst design, together with appropriate termination reactions for synthesis of water-soluble mono-functionalized poly(fluorene)s with controlled molecular weight characteristics and excellent incorporation of protected ethynyl end groups. The organometallic initiator (dppe)Ni(Ph)Br allows polymerization reactions to be carried out in less than 30 seconds, yielding poly(fluorene)s with high $M_n$ and low PDI values. Similar success in the preparation of other conjugated polymer structures is anticipated. After facile deprotection, the mono-functionalized poly(fluorene) react readily with azide-containing organic compounds in nearly quantitative yield, and this chemistry has been used to couple bio-relevant targeting molecules to the polymer chain end. This synthesis strategy results in highly luminescent materials, capable of engaging in biologically-specific binding interactions. In one demonstration, a bio-recognition event is monitored by the extent of energy transfer between a biotin-terminated poly(fluorene) and an organic dye-conjugated streptavidin. FRET between the polymer and dye due to biotin-streptavidin binding gives rise to decreased polymer luminescence and enhanced dye emission and scales with increased concentration of streptavidin-dye. Substantial signal enhancement upon polymer excitation was observed over direct dye excitation. These materials are also active for surface binding; streptavidin-coated beads showed blue luminescence when treated with biotin-functionalized polymer, whereas no emission was evident in a control experiment. These solution and surface recognition capabilities make this material attractive as a component of luminescent bio-assays or for *in vitro* tagging or imaging applications. More generally, a polymer, mono-functionalized with an alkyne moiety as demonstrated herein, is a versatile luminescent reagent platform which can be customized for a particular application by reaction with an appropriate azide starting material. Furthermore, this general scheme is also suitable for fluorene monomers with different substituents at the 9,9'-positions, for applications where a highly-luminescent, well-defined, mono-functionalized material is important, but solubility in organic solvents may be more relevant.

**References**


[1] Hiorns, R. C.; de Bettignies, R.; Leroy, J.; Bailly, S.; Firon, Sentein, C. Khoukh, A.; Preud'homme, H.; Dagron-Lartigue, C. "High Molecular Weights, Polydispersities, And Annealing Temperatures In The Optimization Of Bulk-Heterojunction Photovoltaic Cells Based On Poly(3-Hexylthiophene) Or Poly(3-Butylthiophene)" *Adv. Funct. Mater*. **2006**, *16*, 2263-2273.

[2] Coropceanu, V.; Cornil, J.; da Silva Filho, D. A.; Olivier, Y.; Silbey, R.; Brédas, J.-L. "Charge Transport In Organic Semiconductors" *Chem. Rev*. **2007**, *107*, 926-952.

[3] Brédas, J.-L.; Beljonne, D.; Coropceanu, V.; Cornil, J. "Charge-Transfer And Energy-Transfer Processes In π-Conjugated Oligomers And Polymers: A Molecular Picture" *Chem. Rev*. **2004**, *104*, 4971-5003.

[4] Bellina, F.; Carpita, A.; Rossi, R. "Palladium Catalysts For The Suzuki Cross-Coupling Reaction: An Overview Of Recent Advances" *Synthesis* **2004**, *15*, 2419-2440.

[5] Miyaura, N.; Suzuki, A. "Palladium-Catalyzed Cross-Coupling Reactions Of Organoboron Compounds" *Chem. Rev*. **1995**, *95*, 2457-2483.

[6] Whitcombe, N. J.; Hii, K. K.; Gibson, S. E. "Advances In The Heck Chemistry Of Aryl Bromides And Chlorides" *Tetrahedron* **2001**, *57*, 7449-7476.

[7] Braese, S.; de Meijere, A. *Metal-Catalyzed Cross-Coupling Reactions (2nd Edition)*, Wiley-VCH, 2004, pages 217-315.

[8] (a) Beletskaya, I. P.; Cheprakov, A. V. "The Heck Reaction As A Sharpening Stone Of Palladium Catalysis" *Chem. Rev.* **2000**, *100*, 3009-3066. (b) Alberico, D.; Scott, M. E.; Lautens, M. "Aryl-Aryl Bond Formation By Transition-Metal-Catalyzed Direct Arylation" *Chem. Rev.* **2007**, *107*, 174-238. (c) Heck, R. F. "Palladium-Catalyzed Vinylation Of Organic Halides" *Organic Reactions* **1982**, *27*, 345-390

[9] Farina V.; Krishnamurthy, V.; Scott, W. J. "The Stille Reaction" *Org. React*. **1997**, *50*, 1-652.

[10] Espinet, P.; Echanarren, A. M. "C-C Coupling: The Mechanism Of The Stille Reaction" *Angew. Chem. Int. Ed.* **2004**, *43*, 4707-4734.

[11] (a) Wendt, O. F. "Transmetallation Reactions Involving Group 10 Metals" *Current Organic Chemistry* **2007**, *11*, 1417-1433. (b) Espinet, P.; Echevarren, A. M. "The Mechanisms Of The Stille Reaction" *Angew. Chem. Int. Ed. Engl.* **2004**, *43*, 4704-4734. (c) Stille, J. K. "The Palladium-Catalyzed Cross-Coupling Reactions Of Organotin Reagents With Organic Electrophiles" *Angew. Chem. Int. Ed. Engl.* **1986**, *25*, 508-523.

[12] Sonogashira, K. in "Palladium-Catalyzed Alkynylation" *Handbook of Organopalladium Chemistry for Organic Synthesis; Negishi, E.-i.; de Meijire, A.*; John Wiley & Sons: New York, NY, **2002**, *1*, 493-529.

[13] Negishi, E.-i.; Anastasia, L. "Palladium-Catalyzed Alkynylation" *Chem. Rev.* **2003**, *103*, 1979-2017.

[14] Chinchilla, R.; Najera, C. "The Sonogashira Reaction: A Booming Methodology In Synthetic Organic Chemistry" *Chem. Rev.* **2007**, *107*, 874-922.

[15] Gaylord, B. S.; Heeger, A. J.; Bazan, G. C. "DNA Hybridization Detection With Water-Soluble Conjugated Polymers And Chromophore-Labeled Single-Stranded DNA" *J. Am. Chem. Soc.* **2003**, *125*, 896-900.

[16] Elsenbaumer, R. L.; Jen, K. Y.; Oboodi, R. "Processible and environmentally stable conducting polymers" *Synth. Met.* **1986**, *15*, 169–174.
[17] Xin, H.; Kim, F. S.; Jenekhe, S. A. "Highly Efficient Solar Cells Based on Poly(3-butylthiophene) Nanowires" *J. Am. Chem. Soc.* **2008**, *130*, 5424-5425.
[18] Iovu, M. C.; Shiena, E. E.; Gil, R. R.; McCullough, R. D. "Experimental Evidence For The Quasi-"Living" Nature Of The Grignard Metathesis Method For The Synthesis Of Regioregular Poly(3-Alkylthiophenes)" *Macromolecules* **2005**, *38*, 8649-8656.
[19] Jeffries-EL, M.; Sauve, G.; McCullough, R. D**. "**In-Situ End-Group Functionalization of Regioregular Poly(3-alkylthiophene) Using the Grignard Metathesis Polymerization Method**"** *Adv. Mater.* **2004**, *16*, 1017-1019.
[20] Amatore, C.; Jutand, A. "Rates and Mechanism of Biphenyl Synthesis Catalyzed by Electrogenerated Coordinatively Unsaturated Nickel Complexes" *Organometallic*s, **1988**, *7(10)*, 2203-2214.
[21] (a) Iovu, M.; Sheina, E.; Gil, R.; McCullough, R. "Experimental Evidence for the Quasi-"Living" Nature of the Grignard Metathesis Method for the Synthesis of Regioregular Poly(3-alkylthiophenes)" *Macromolecules*, **2005**, *38*, 8649-8656 (b) Beryozkina, T.; Senkovskky, V.; Kaul, E.; Kiriy, A. "Kumada Catalyst-Transfer Polycondensation of Thiophene-Based Oligomers: Robustness of a Chain-Growth Mechanism" *Macromolecules*, **2008**, *41*, 7817-7823.
[22] Achord, B.; Rawlins, J. "Evidence of Ni(0) Complex Diffusion during Grignard Metathesis Polymerization of 2,5-Dibromo-3-hexylthiophene" *Macromolecules*, **2009**, *42(22)*, 8634-8639.
[23] Y. Mao, Y. Yang and B. Lucht, "Regiocontrolled synthesis of poly(3-alkylthiophene)s by Grignard metathesis" *J. Poly Sci. A*, **2004***, 41(21)*, 5538-5547.
[24]
[25] (a) Odian, G. *Principles of Polymerization*, 4th Ed.; Wiley Interscience: Hoboken, NJ, 2004 (b) Croucher, T. G.; Wetton, R. E. "Synthesis of Narrow Polydispersity Polytetrahydrofuran" *Polymer*, **1976**, *17*, 205-211. (c) Cunningham, M F. "Living/Controlled Radical Polymerization in Dispersed Phase Systems" *Prog. Polym. Sci.*, **2002**, *27*, 1039-1067.
[26] (a) Jerries-EL, M.; Sauvé, G.; McCullough, R. "In-Situ End-Group Functionalization of Regioregular Poly(3-alkylthiophene) using the Grignard Metathesis Polymerization Method" *Adv. Mater.*, **2004***, 16(12),* 1017-1019 (b) Jerries-EL, M.; Sauvé, G.; McCullough, R. "Facile Synthesis of End-Functionalized Regioregular Poly(3-alkylthiophene)s via Modified Grignard Metathesis Reaction" *Macromolecules*, **2005**, *38*, 10346-10352.
[27] Miyakoshi, R.; Yokoyama, A.; Yokozawa, T. *J. Am. Chem. Soc.* **2005**, *127*, 17542-17547.
[28] Huang, L.; Wu, S.; Qu, Y.; Geng, Y.; Wang, F. *Macromolecules* **2008**, *41*, 8944-8947.
[29] Wang, F.; Bazan, G.C. *J. Am. Chem. Soc.* **2006**, *128*, 15786-15792.
[30] French, A.C.; Thompson, A.L.; Davis, B.G. *Angew. Chem. Int. Ed.* **2009**, *48*, 1248-1252.
[31] Shao, M.; Dongare, P.; Dawe, L.N.; Thompson, D.W.; Zhao, Y. *Org. Lett.* **2010**, *12*, 3050-3053.
[32] Wissner, A.; Kohler, C.A.; Goldstein, B.M. *J. Med. Chem.* **1986**, *29*, 1315-1319.
[33] Grieco, P.A.; Parker, D.T. *J. Org. Chem.* **1988**, *53*, 3658-3662.
[34] Grell, M.; Bradley, D.D.C.; Long, X.; Chamberlain, T.; Inbasekaran, M.; Woo, E.P.; Soliman, M. *Acta. Polym.* **1998**, *49*, 439-444.
[35] Huang, F.; Zhang, Y.; Liu, M.S.; Jen, A.K.Y. *Adv. Funct. Mater.* **2009**, *19*, 2457-2466.
[36] Pu, K.Y.; Fang, Z.; Liu, B. *Adv. Funct. Mater.* **2008**, *18*, 1321-1328.

[37] Thomas, K.R.J.; Lin, J.T.; Lin, Y.Y.; Tsai, C.; Sun, S.S. *Organometallics* **2001**, *20*, 2262-2269.
[38] Scherf, U.; List, E.J.W. *Adv. Mater.* **2002**, *14*, 477-487.
[39] Zhu, B.; Han, Y.; Sun, M.; Bo, Z. *Macromolecules* **2007**, *40*, 4494-4500.
[40] Qin, C.; Wu, X.; Gao, B.; Tong, H.; Wang, L. *Macromolecules* **2009**, *42*, 5427-5429.
[41] Meldal, M.; Tornoe, C.W. *Chem. Rev.* **2008**, *108*, 2952-3015.
[42] Kolb, H.C.; Finn, M.G.; Sharpless, K.B. *Angew. Chem. Int. Ed.* **2001**, *40*, 2004-2021.
[43] Amblard, F.; Cho, J.H.; Schinazi, R.F. *Chem. Rev.* **2009**, *109*, 4207-4220.
[44] Rostovtsev, V.V.; Green, L.G.; Fokin, V.V.; Sharpless, K.B. *Angew. Chem. Int. Ed.* **2002**, *41*, 2596-2599.
[45] Maji, M.S.; Pfeifer, T.; Studer, A. *Chem. Eur. J.* **2010**, *16*, 5872-5875.
[46] Shi, W.; Dolai, S.; Averick, S.; Fernando, S.S.; Saltos, J.A.; L'Amoreaux, W.; Banerjee, P.; Raja, K. *Bioconjugate Chem.* **2009**, *20*, 1595-1601.
[47] Green, N.M. *Methods Enzymol.* **1990**, *184*, 51-67.
[48] Bernier, S.; Garreau, S.; Bera-Aberem, M.; Gravel, C.; Leclerc, M. *J. Am. Chem. Soc.*, **2002**, *124*, 12463-12468.
[49] Ji, E.; Wu, D.; Schanze, K.S. *Langmuir*, **2010**, *26*, 14427-14429.
[50] Wilchek, M.; Bayer, E.A. *Methods Enzymol.* **1990**, *184*, 5-13.
[51] Wilchek, M.; Bayer, E.A. *Anal. Biochem.* **1988**, *171*, 1-32.
[52] Obtained from Quanta Biodesign, http://quantabiodesign.com
[53] Lapin, N.A.; Chabal, Y.J. *J. Phys. Chem. B* **2009**, *25*, 8776-8783.
[54] Forster, T. *Naturwissenschaften* **1946**, *33* 166-175.
[55] Huebsch, N.D.; Mooney, D.J. *Biomaterials*, **2007**, *28*, 2424-2437.
[56] Campbell, R.E. *Anal. Chem.* **2009**, *81*, 5972-5979.
[57] Forster, T. *Discuss. Faraday Soc.* **1959**, *27*, 7-17.
[58] Laintinen, O.H.; Nordlund, H.R.; Hytonen, V.P.; Kulomaa, M.S. *Trends Biotechnol.* **2007**, *25*, 269-277.
[59] Hu, S.; Yang, H.; Cai, R.; Liu, Z.; Yang, X. *Talanta* **2009**, *80*, 454-458.
[60] Bayer, E.A.; Wilchek, M. *J. Chromatogr.* **1990**, *510*, 3-11.